Inorg. Chem. **2003**, *42*, 3709–3711

A Novel Organic–Inorganic Hybrid Based on a Dinuclear Copper Complex Supported on a Keggin Polyoxometalate

Santiago Reinoso, Pablo Vitoria, Luis Lezama,* Antonio Luque, and Juan M. Gutiérrez-Zorrilla*

Departamento de Química Inorgánica, Facultad de Ciencias, Universidad del País Vasco, P.O. Box 644, E-48080 Bilbao, Spain

Received February 24, 2003

The autoassembly process of copper–oxalate dimers and Keggin type polyoxometalates leads to the first example of a new family of organic–inorganic hybrids, $K_{14}[\{Cu_2(bpy)_2(\mu\text{-ox})\}\{SiW_{11}O_{39}Cu(H_2O)\}]_2[SiW_{11}O_{39}Cu(H_2O)]\cdot\sim 55H_2O$. This compound crystallizes in the monoclinic space group *C*2/*m*, $a = 37.932(6)$ Å, $b = 21.303(3)$ Å, $c = 12.546(2)$ Å, $\beta = 106.16(1)°$, $Z = 2$. The crystal structure reveals the presence of a polymeric hybrid built up of alternating dimer and polyoxometalate entities.

Hybrid organic−inorganic compounds have attracted an increasing interest in recent years due to the possibility of combining the different characteristics of the components to get unusual structures, properties, or applications.

Polyoxometalates (POMs) are one of the most widely used inorganic components.[1] This fact lies in the extreme variability of compositions, molecular characteristics, properties, and applications.[2] In this way, the functionalization of POMs with transition metal (TM) complex moieties constitutes an emerging area. To date, several hybrid compounds based on vanadium[3] and molybdenum[4] isopolyanions have been reported, but in contrast, the role of Keggin heteropolyanions as the inorganic component has not been so extensively studied.[5]

Currently, we are interested in exploring the applicability of Keggin-POMs and TM−oxalate complexes in the preparation of new hybrid compounds. The present paper reports the synthesis, crystal structure, and magnetic properties of the first example of this family, $K_{14}[\{Cu_2(bpy)_2(\mu\text{-ox})\}\{SiW_{11}O_{39}Cu(H_2O)\}]_2[SiW_{11}O_{39}Cu(H_2O)]\cdot\sim 55H_2O$ (**1**). The interest in supporting TM−oxalate complexes, which have been extensively studied in magnetostructural research works,[6] on Keggin-POMs lies in the possibility of tuning the magnetic properties due to their high dependence on the nature and spatial disposition of the ligands.[7] Moreover, the dimers could play the role of structure-directing agents, so that the Keggin-POMs could be templated to lead to opened structures with tailorable pore shapes and sizes.[8]

In contrast to the big majority of the TM complex−POM compounds reported in the literature, which are synthesized by hydrothermal techniques, we have made use of the more predictable classical open-air techniques for the synthesis of **1**, which is formed by an autoassembly process of the *in situ* generated building blocks.

* Authors to whom correspondence should be addressed. E-mail: qipguloj@lg.ehu.es (J.M.G.-Z.), qipledil@lg.ehu.es (L.L.). Fax: +34 944 64 85 00.

(1) (a) *Polyoxometalate Chemistry for Nanocomposite Design*; Pope, M. T., Yamase, T., Eds.; Kluwer: Dordrecht, 2002. (b) *Polyoxometalates: From Topology via Self-Assembly to Applications*; Pope, M. T., Müller, A., Eds.; Kluwer: Dordrecht, 2001. (c) *Polyoxometalates: From Platonic Solids to Antiretroviral Activity*; Pope, M. T., Müller, A., Eds.; Kluwer: Dordrecht, 1994.

(2) (a) Weinstock, I. A. *Chem. Rev.* **1998**, *98*, 113. (b) Kozhevnikov, I. V. *Chem. Rev.* **1998**, *98*, 171. (c) Mizuno, N.; Misono, M. *Chem. Rev.* **1998**, *98*, 199. (d) Fukuda, N.; Yamase, T.; Tajima, Y. *Biol. Pharm. Bull.* **1999**, *22*, 463. (e) Rhule, J. T.; Hill, C. L.; Judd, D. A.; Schinazi, R. F. *Chem. Rev.* **1998**, *98*, 327. (f) Kortz, U.; Isber, S.; Dickman, M. H.; Ravot, D. *Inorg. Chem.* **2000**, *39*, 2915. (g) Müller, A.; Beugholt, C.; Kögerler, P.; Bögge, H.; Bud'ko, S.; Luban, M. *Inorg. Chem.* **2000**, *39*, 5176. (h) Clemente-Juan, J. M.; Coronado, E. *Coord. Chem. Rev.* **1999**, *193*−*195*, 361. (i) Clemente-León, M.; Coronado, E.; Delhaes, P.; Gómez-García, C. J.; Mingolaud, C. *Adv. Mater.* **2001**, *13*, 574. (j) Coronado, E.; Gómez-García, C. J. *Chem. Rev.* **1998**, *98*, 273. (k) Yamase, T. *Chem. Rev.* **1998**, *98*, 307. (l) Ouahab, L. *Coord. Chem. Rev.* **1998**, *178*−*180*, 1501.

(3) (a) Finn, R. C.; Sims, J.; O'Connor, C. J.; Zubieta, J. *J. Chem. Soc., Dalton Trans.* **2002**, 159. (b) Laduca, R. L., Jr.; Rarig, R. S., Jr.; Zubieta, J. *Inorg. Chem.* **2001**, *40*, 607. (c) Do, J.; Jacobson, A. J. *Inorg. Chem.* **2001**, *4*, 598. (d) Hagrman, P. J.; Zubieta, J. *Inorg. Chem.* **2001**, *40*, 2800. (e) Zheng, L.-M.; Wang, X.; Wang, Y.; Jacobson, A. J. *J. Mater. Chem.* **2001**, *11*, 1100.

(4) (a) Lu, C.-Z.; Wu, C.-D.; Zhuang, H.-H.; Huang, J.-S. *Chem. Mater.* **2002**, *14*, 2649. (b) Rarig, R. S., Jr.; Hagrman, P. J.; Zubieta, J. *Solid State Sci.* **2002**, *4*, 77. (c) Rarig, R. S., Jr.; Zubieta, J. *J. Solid State Chem.* **2002**, *167*, 370. (d) Hagrman, P. J.; Zubieta, J. *Inorg. Chem.* **2000**, *39*, 5218;

(5) (a) Luan, G.; Li, Y.; Wang, S.; Wang, E.; Han, Z.; Hu, C.; Hu, N.; Jia, H. *Dalton Trans.* **2003**, 233. (b) Yuan, M.; Li, Y.; Wang, E.; Lu, Y.; Hu, C.; Hu, N.; Jia, H. *J. Chem. Soc., Dalton Trans.* **2002**, 2916. (c) Yang, W.; Lu, C.; Zhuang, H. *J. Chem. Soc., Dalton Trans.* **2002**, 2879. (d) Yan, B.; Xu, Y.; Bu, X.; Goh, N. K.; Chia, L. S.; Stucky, G. D. *J. Chem. Soc., Dalton Trans.* **2001**, 2009. (e) Bu, W.-M.; Ye, L.; Yang, G.-Y.; Gao, J.-S.; Fan, Y.-G.; Shao, M.-C.; Xu, J.-Q. *Inorg. Chem. Commun.* **2001**, *4*, 1.

(6) (a) Coronado, E.; Galán-Mascarós, J. R.; Giménez-Saiz, C.; Gómez-García, J.; Ruiz-Pérez, C.; Triki, S. *Adv. Mater.* **1996**, *8*, 737. (b) Kahn, O. *Molecular Magnetism*; VCH: New York, 1993.

(7) (a) Cano, J.; Alemany, P.; Álvarez, S.; Verdaguer, M.; Ruiz, E. *Chem. Eur. J.* **1998**, *4*, 476. (b) Álvarez, S.; Julve, M.; Verdaguer, M. *Inorg. Chem.* **1990**, *29*, 4500.

(8) (a) Ugalde, M.; Gutiérrez-Zorrilla, J. M.; Vitoria, P.; Luque, A.; Wèry, A. S. J.; Román, P. *Chem. Mater.* **1997**, *9*, 2869. (b) Vitoria, P.; Ugalde, M.; Gutiérrez-Zorrilla, J. M.; Román, P.; Luque, A.; San Felices, L.; García-Tojal, J. *New J. Chem.* **2003**, *27*, 399.

10.1021/ic034203a CCC: $25.00
Published on Web 05/20/2003

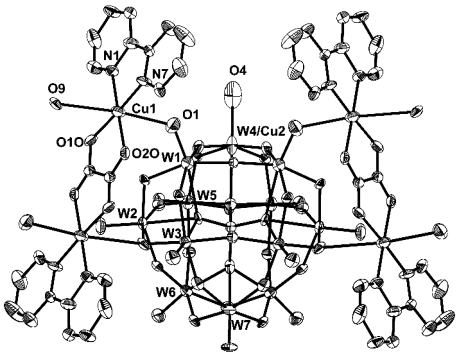

Figure 1. ORTEP view of the hybrid polyanion together with atom labeling.

The crystal structure[9] of **1** consists of corrugated chains built up of alternating $[Cu_2(bpy)_2(\mu\text{-ox})]^{2+}$ and $[\alpha\text{-}SiW_{11}O_{39}Cu(H_2O)]^{6-}$ building blocks, free $[\alpha\text{-}SiW_{11}O_{39}Cu(H_2O)]^{6-}$ POMs, potassium cations, and hydration water.

The $[\alpha\text{-}SiW_{11}O_{39}Cu(H_2O)]^{6-}$ anion consists of a central SiO_4 tetrahedron surrounded by four vertex-sharing M_3O_{13} trimers that result from the association of three edge-sharing MO_6 octahedra in such a way that the ideal polyanion has C_s symmetry. The copper atom Cu2 is disordered over the whole polyanion, but there is a preferential position on the W4 site (56%). The M−O bond distances are in the ranges 2.16−2.46 Å for central oxygen atoms, 1.85−2.01 Å for bridging oxygen atoms, and 1.64−1.79 Å for terminal oxygen atoms, while the Cu2−O4w is 2.02 Å. This copper atom is connected to the two mirror plane related dimmers via bridging oxygen−tungsten−terminal oxygen links (Cu2−O11−W1−O1−Cu1), while the copper atom of the free POM is disordered over the 12 possible positions (Figure 1).

The centrosymmetric $[Cu_2(bpy)_2(\mu\text{-ox})]^{2+}$ dimer is made of two copper atoms bridged by an oxalate ion in the usual bis(bidentate) fashion with a Cu−Cu distance of 5.15 Å. The copper atoms are involved in CuN_2O_4 chromophores in tetragonally elongated octahedral environments. The equatorial coordination positions are occupied by two oxalate oxygen atoms and two bipyridine nitrogen atoms with regular Cu−O and Cu−N distances around 1.97 Å. The dimers are supported over W_3O_{13} trimers in such a way that the apical positions of the copper atoms are occupied, on one hand, by the terminal oxygen O1 of the W1 octahedron and, on the other hand, by the bridging oxygen atom O9 belonging to W2 and W3 octahedra. The Cu1−O1 and Cu1−O9 distances are significantly different, 2.54 and 2.94 Å, respectively, so that the dimer may be considered as coordinated to terminal oxygens and semicoordinated to bridging oxygen atoms.

The hybrid chains run antiparallely along the *b* axis, and the connection between them is made by potassium cations, leading to cavities that are filled by free $[\alpha\text{-}SiW_{11}O_{39}Cu(H_2O)]^{6-}$ anions. In this way, layers of hybrid chains and free POMs are formed (Figure 2). These layers are placed parallel to the *xy* plane, and the connection between them is made by π interactions between the bipyridine ligands. The bipyridine planes are almost parallel and offset displaced, the interplanar, intercentroidal, and offset distances being 3.48, 3.94, and 1.85 Å respectively. This type of layer packing along the *c* axis leads to an open structure with trapezoidal tunnels of 14 × 5 Å ($\alpha \sim 120°$) dimensions where disordered hydration water is located.

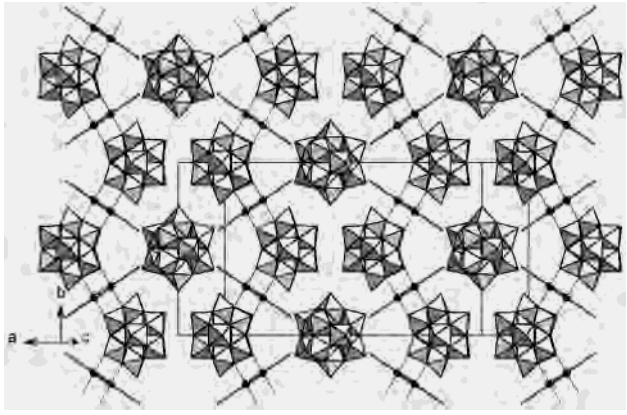

Figure 2. Packing of the structure showing the hybrid chains and the free polyanions. Potassium cations and water are omitted for clarity.

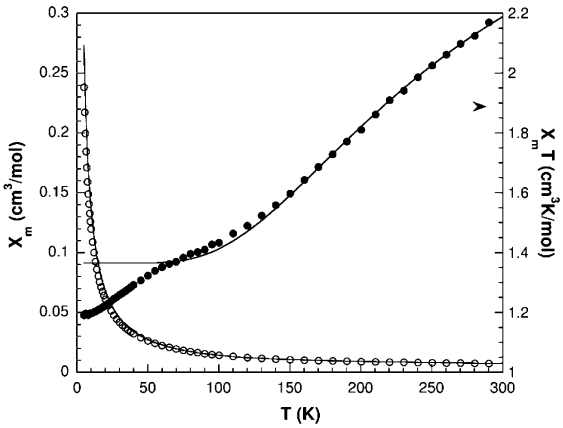

Figure 3. Thermal evolution of the magnetic susceptibility and $\chi_m T$ product. Continuous lines correspond to the best least-squares fit of the high-temperature data ($T > 100$ K).

Plots showing the thermal evolution of the magnetic molar susceptibility and the $\chi_m T$ product, being $\chi_m T = \mu_{eff}^2/8$, are shown in Figure 3. The room temperature $\chi_m T$ value (0.749 $cm^3 \cdot K \cdot mol^{-1}$) is substantially lower than that expected for seven uncoupled Cu(II) ions (2.625 $cm^3 \cdot K \cdot mol^{-1}$, considering $g = 2$). This fact indicates the predominance of antiferromagnetic interactions in compound **1**, as confirmed by the rapid decrease of the effective magnetic moment with decreasing temperature (from 4.18 μ_B at 300 K to 3.09 μ_B at 5 K). Moreover, the exchange coupling must be certainly strong considering that Curie−Weiss behavior is not observed even at the high temperatures on the reciprocal susceptibility curve.

A priori, the magnetic behavior of this compound must be dominated by the presence of two oxalate-bridged Cu(II) dimers per formula unit. It is well-known that μ-oxalatodicopper(II) complexes exhibit strong antiferromagnetic

(9) Crystal data for **1**: crystal dimensions 0.56 × 0.07 × 0.01 mm, monoclinic, *C*2/*m*; $a = 37.932(6)$ Å, $b = 21.303(3)$ Å, $c = 12.546(2)$ Å, $\beta = 106.16(1)°$, $V = 9737(3)$ Å^3, $Z = 2$, $\rho_{calc} = 3.688$ Mg·m^{-3}, $2\theta_{max} = 60°$, Enraf Nonius CAD 4 diffractometer, $T = 295(2)$ K, λ(Mo Kα) = 0.71073 Å, $\mu = 20.588$ mm^{-1}, 15207 reflections, 14586 unique reflections, 618 parameters, R1 = 0.0704 [$I > 2\sigma(I)$], wR2 = 0.199 (all data), maximum residual electron density 4.893 e·Å^{-3}.

interactions.[6b,7] Under this situation, the $d_{x^2-y^2}$ Cu magnetic orbital is directed toward the oxalate σ orbitals, the antiferromagnetic contribution is therefore maximized, and J values near -200 cm^{-1} are usually observed (calculated with the Heisenberg spin Hamiltonian $\mathbf{H} = (-2J)\mathbf{SA}\cdot\mathbf{SB}$). However, the complexity of the crystal structure, with three different positions for the copper(II) ions, makes the analysis of the observed magnetic behavior difficult. For instance, in spite of the presence of strong antiferromagnetic interactions, no relative maximum is observed on the susceptibility versus temperature curve: it is possible that the expected maximum is reached out of the measured temperature range, but it is also possible that the maximum is masked by the contributions of Cu(II) ions sited in the POM clusters. A purely paramagnetic behavior has to be expected for free copper-monosubstituted POMs, but it is not so obvious for the $[SiW_{11}O_{39}Cu(H_2O)]^{6-}$ subunits linked by the copper−oxalate dimers. In order to obtain more information about the role played by the POM clusters in the observed magnetic behavior, we have tried to fit the experimental data by using the Bleaney−Bowers equation for a dinuclear copper(II) complex,[10] modified to take into account the presence of two dimeric and three monomeric copper entities per formula unit. No reasonable fit could be obtained over the whole experimental curve, but taking only the data above 100 K a relatively good fit could be achieved (solid lines in Figure 3) with the adjustable parameters $J = -172$ cm^{-1} and $g = 2.12$. Even if the fit is not completely satisfactory, the calculated J value is in good agreement with the structural characteristics, and it can be considered as a rather good approximation. The discrepancy between experimental and calculated data at low temperatures is also relevant, and it suggests that the oxalate dimers are not magnetically isolated. Attempts to improve the fit including the presence of interdimeric interactions, by means of a J' exchange parameter treated in the molecular field approximation,[11] do not lead to better results.

The temperature dependence of the X-band spectra is illustrated in Figure 4. As expected, the room temperature spectra are rather complex, due to the presence of different Cu(II) centers. However, when cooling down the resolution is considerably improved, apparently as a result of the signal narrowing induced by the increasing spin−lattice relaxation time. At 4.2 K, the spectrum is characteristic of an isolated Cu(II) chromophore with an axial **g** tensor. It clearly shows, on the parallel region, the hyperfine splitting originated by a spin doublet $S = {}^1/_2$ interacting with a single $I = {}^3/_2$ nucleus. Obviously, this signal must be originated by the copper substituted POMs.

The thermal dependence of the Q-band spectra (Figure 4) is more significant. At room temperature, two different signals are clearly detected. One of them, with axial resolution and hyperfine splitting, is the same identified on the X-band low-temperature spectra. The other one is a broad signal, centered at about 11500 G, that rapidly disappears as the temperature is lowered. Considering this behavior, the broad signal can be attributed to the oxalate copper dimers, the strong antiferromagnetic interaction being responsible for the decreasing intensity with decreasing temperature. However, the observed signal does not correspond to an isolated triplet $S = 1$ state, and therefore a non-negligible magnetic interaction has to be established between dimers. The exchange pathway must involve the $[SiW_{11}O_{39}Cu(H_2O)]^{6-}$ units that link the $[Cu_2(bpy)_2(\mu\text{-ox})]^{2+}$ entities to build infinite chains. The participation of the Cu(II) ion inside the POM cluster in the magnetic exchange cannot be a priori disregarded, even if it seems not very probable. New studies on related systems are in progress in order to clarify this point.

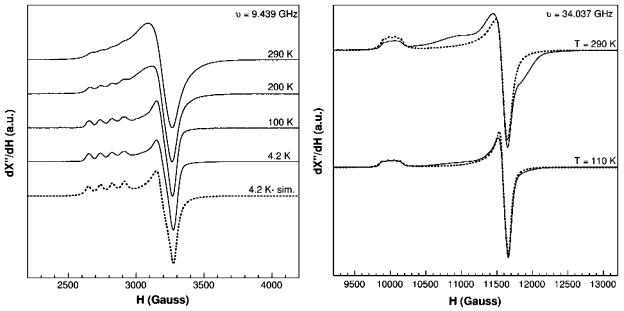

Figure 4. Left: Temperature dependence from 4.2 K up to 290 K of the powder X-band EPR spectra. Right: Q-band EPR powder spectra. Dotted lines correspond to simulated spectra for an isolated Cu(II) ion.

Table 1. Spin Hamiltonian Parameters for Isolated Cu(II) Ions in **1**

	$g_{\parallel}$	$g_{\perp}$	$A_{\parallel}$ ($\times 10^{-4}$ cm^{-1})	$A_{\perp}$ ($\times 10^{-4}$ cm^{-1})
X-band (4.2 K)	2.425	2.090	100	28
Q-band (290 K)	2.426	2.095	90	28
Q-band (110 K)	2.430	2.093	95	28

With respect to the axial signal originated by isolated Cu(II) centers, the spin Hamiltonian parameters were estimated by comparison of the experimental spectra with those obtained by a computer simulation program working at the second order of the perturbation theory. The parameters were then optimized by the trial and error method. The calculated spectra are the dotted lines in Figure 4, and the obtained values are given in Table 1. The main values of the **g** and **A** tensors are typical of octahedrally coordinated Cu(II) ions with the unpaired electron on the $d_{x^2-y^2}$ orbital.

Acknowledgment. This work was supported by MEC (MAT2002-03166). S.R. thanks Gobierno Vasco.

Supporting Information Available: Detailed experimental procedures, bond distances and angles, figures depicting the ORTEP view, packing of the structure, trapezoidal tunnels, π-interactions, χ_m and $\chi_m T$ vs T plots, and EPR powder spectra. An X-ray crystallographic file, in CIF format. This material is available free of charge via the Internet at http://pubs.acs.org.

IC034203A

(10) Bleany, B.; Bowers, K. D. *Proc. R. Soc. London, Ser. A* **1952**, *214*, 451.
(11) Carlin R. L. *Magnetochemistry*; Springer: Berlin, 1986.